

# Measurement and Correlation of Protein Adsorption with Mixed-Mode Adsorbents Taking into Account the Influences of Salt Concentration and pH

Dong Gao, Dong-Qiang Lin, and Shan-Jing Yao\*

Department of Chemical and Biochemical Engineering, Zhejiang University, Hangzhou 310027, People's Republic of China

The isotherm adsorption behavior of bovine serum albumin on the mixed-mode cellulose–stainless steel powder composite adsorbent with benzylamine as the functional ligand (named Cell-SSP-BA) was measured using batch experiments. Four separate adsorbents with different ligand densities were studied under varying salt concentrations and pH. The mixed-mode adsorbent Cell-SSP-BA showed the salt-tolerant and pH-dependent properties for protein binding. An empirical modification of the Langmuir equation has been proposed to describe the effects of both salt concentration and pH on the isotherm behaviors of mixed-mode adsorption. The results indicated that the modified Langmuir equation could correlate the protein adsorption at different salt concentrations and pH with only one set of parameters.

## Introduction

Chromatography technology has been used widely for biomolecule separation due to its high-resolution power. For normal chromatographic techniques, such as ion-exchange chromatography (IEC), hydrophobic interaction chromatography (HIC), affinity chromatography (AC), and size exclusion chromatography (SEC), protein separation is dependent mainly on their single biological and physicochemical properties such as net charge, hydrophobicity, biospecific characteristics, or molecular size. To improve separation effects and avoid nonspecific adsorptions, many studies on multi-mode chromatography have been published.<sup>1–5</sup> In 1997, Burton et al.<sup>5</sup> reported a mixed-mode technique, combining hydrophobic and electrostatic interactions for chymosin separation, which showed a specific property of salt-independent adsorption. Such salt-independent adsorption methods with mixed-mode ligands appear to offer particular potential and have several advantages for protein separation,<sup>4</sup> especially for expanded bed adsorption (EBA) applications primarily intended to capture target proteins directly from high ionic strength feedstock without pre-dilution.<sup>4,6</sup>

The ligands of mixed-mode adsorbents have both a hydrophobic interaction group and an electrostatic interaction group. Such structures cause a protein adsorption behavior to be mixed-mode functions and complicated. At low ionic strength the charged group of ligand implements the ion exchange adsorption of the target protein,<sup>4</sup> and as ionic strength increases, the aromatic ring of ligand allows hydrophobic interaction to occur in salt-tolerant adsorption. High binding capacities can be achieved at moderate conductivities of from (15 to 30)  $\text{mS}\cdot\text{cm}^{-1}$  without additional dilution steps in advance, while the desorption can be induced with electrostatic charge repulsion and accomplished by changing the pH of the mobile phase across the isoelectric point of the protein. It is obvious that mixed-mode protein adsorption has a strong dependence on both salt concentration and pH, and more detailed studies on the

adsorption mechanism are necessary. However, the literature on mixed-mode chromatography has been largely focused on application.<sup>5–7</sup> The limitation of the understanding of adsorption mechanisms most certainly impedes the application of mixed-mode adsorption. Ghose et al.<sup>8</sup> reported a characterization of protein interactions with hydrophobic charge induction chromatography and correlated the protein adsorption isotherms over a range of pH values and salt concentrations with a modified Langmuir isotherm equation.

In our previous work,<sup>9–13</sup> a series of mixed-mode adsorbents (named Cell-SSP-BA) with regenerated cellulose as the backbone and benzylamine as the functional ligand were prepared and studied using different ligand densities. In this work, using bovine serum albumin (BSA) as the model protein, the binding behaviors of Cell-SSP-BA are determined under varying operation conditions. Some important factors influencing protein adsorption such as salt concentration, pH, and ligand density are studied systematically. Additionally, a Langmuir isotherm equation modification is used to correlate the effects of salt concentration and pH on the protein isotherm adsorption.

## Experimental Section

**Materials.** Bovine serum albumin (BSA) (A-7030), with a MW of 67 kDa and a theoretical pI of 4.9, was obtained from Sigma (Milwaukee, WI). Other reagents were of analytical reagent grade and were purchased from local suppliers. Cell-SSP-BA mixed-mode adsorbents with benzylamine as the functional ligand were prepared using a method published previously<sup>9–13</sup> and named Cell-SSP-BA-1, Cell-SSP-BA-2, Cell-SSP-BA-3, and Cell-SSP-BA-4 with different ligand densities of ( $120 \pm 2$ ,  $103 \pm 1$ ,  $65 \pm 2$ , and  $49 \pm 1$ )  $\mu\text{mol}\cdot\text{mL}^{-1}$ , respectively.

**Procedures.** The adsorption isotherms of BSA at different pH values and salt concentrations were determined using batch experiments. The adsorbents with different ligand densities were drained after being washed in the equilibration buffer under investigation, and 5  $\text{mg}\cdot\text{mL}^{-1}$  BSA stock was prepared in each of the buffers at different salt concentrations and pH values.

\* Corresponding author. Tel: +86-571-87951982. E-mail: yaosj@zju.edu.cn.

**Table 1. Experimental Results of BSA Adsorption with Cell-SSP-BA at Different Sodium Chloride Concentrations**

$L^a$	0 mol·L <sup>-1</sup>		0.25 mol·L <sup>-1</sup>		0.35 mol·L <sup>-1</sup>		0.50 mol·L <sup>-1</sup>	
	$C$	$Q$	$C$	$Q$	$C$	$Q$	$C$	$Q$
$\mu\text{mol}\cdot(\text{mL of gel})^{-1}$	$\text{mg}\cdot\text{mL}^{-1}$	$\text{mg}\cdot(\text{mL of gel})^{-1}$	$\text{mg}\cdot\text{mL}^{-1}$	$\text{mg}\cdot(\text{mL of gel})^{-1}$	$\text{mg}\cdot\text{mL}^{-1}$	$\text{mg}\cdot(\text{mL of gel})^{-1}$	$\text{mg}\cdot\text{mL}^{-1}$	$\text{mg}\cdot(\text{mL of gel})^{-1}$
120	0.20	34.9	0.40	35.4	0.42	33.7	0.54	33.5
	0.46	56.7	0.46	56.7	1.49	52.7	1.53	43.5
	0.96	75.8	1.39	67.7	2.35	57.9	2.40	49.1
	2.09	87.3	2.57	72.9	3.18	61.7	3.29	51.7
	3.18	88.1	3.42	79.2	3.72	69.0	4.02	49.5
	3.80	90.4	3.94	79.2	4.12	68.6	4.34	50.3
103	0.20	34.5	0.43	34.3	0.94	36.6	1.15	29.6
	0.43	57.1	0.64	51.5	1.85	49.7	2.08	36.6
	1.09	73.4	1.85	62.5	2.56	48.7	2.91	39.3
	2.32	80.6	2.54	69.8	3.27	56.3	3.66	40.3
	3.50	81.9	3.53	69.7	3.90	58.7	4.14	43.2
	4.55	84.9	4.57	68.1	4.21	58.3	4.41	44.5
65	0.38	33.9	1.04	34.0			1.37	21.5
	0.69	50.1	1.36	41.4			1.85	26.7
	1.29	63.8	1.95	45.8			2.27	26.7
	2.33	70.0	2.68	51.3			2.72	30.2
	3.23	73.5	3.29	55.1			3.29	31.6
	3.67	73.6	3.59	56.9			3.55	34.4
49	0.54	33.4	0.80	22.0			1.72	17.1
	0.77	52.9	0.93	31.1			2.14	23.3
	1.77	60.5	1.15	34.7			2.68	24.7
	2.79	66.2	1.63	41.2			3.03	29.0
	3.66	67.2	2.08	46.2			3.45	27.6
	4.04	72.0	2.38	46.6			3.56	31.8

<sup>a</sup>  $L$  means ligand density.

Different adsorbent masses were added, which were prepared gravimetrically using an analytical balance with an accuracy of  $\pm 0.1$  mg, respectively, to identical buffered 15 mL BSA solutions. The adsorption experiments were conducted at ( $25 \pm 0.1$ ) °C for 10 h in a shaking incubator. After adsorption equilibrium, the adsorbents were separated, and the supernatant was analyzed for protein concentration with a UV detector (Ultrospec 3300, Amersham Biosciences, Sweden) at 280 nm. The adsorbed protein mass was calculated from the mass balance of initial and final protein concentration in the solution. The protein concentrations were analyzed in triplicate, and the experimental errors were within  $\pm 5\%$ . Then the isotherms at different salt concentrations and pH were obtained, and the curves were fitted by the Langmuir equation and a modified equation.

## Results and Discussion

As mentioned above, solution ionic strength and pH are two important factors relative to mixed-mode adsorbents for protein adsorption. The salt-tolerant properties are dependent on the ligand chemistry of mixed-mode adsorbents. Some mixed-mode ligands exhibit total independence of ionic strength (e.g., hydrophobic charge induction chromatography),<sup>8,14</sup> and some evidence slight salt-dependence (e.g., Fastline PRO).<sup>6</sup> The strong ion exchange adsorbent with hydrophobic backbones (e.g., POROS 50 HS)<sup>4,15</sup> also exhibit some amount of salt-tolerant properties. In addition, the ligand density also plays an important role in the selectivity and binding capacity. A higher density of functional groups on the adsorbent leads to a higher protein binding capacity.<sup>16</sup> Therefore, in the present work the effect of ligand density had to be investigated along with the effects of salt concentration and pH.

The Langmuir equation is the most widely adopted form for the correlation of protein adsorption equilibrium.<sup>17,18</sup> However, the parameters of Langmuir equation are not implicit functions of pH and ionic strength, both of which are of importance for

mixed-mode adsorption. To describe the influence of salt concentration on the equilibrium, Hu et al.<sup>19</sup> used the Langmuir model with an empirical relation between the equilibrium constant and the salt concentration while James and Do<sup>20</sup> used the competitive Langmuir–Freundlich isotherm. The Steric Mass Action model is another theoretical model which incorporates the influence of salt concentration.<sup>21</sup> In the literature, modeling pH effects on adsorption behavior have received insufficient attention, and only a few investigations on this topic have been reported.<sup>8,22</sup>

The effect of salt concentration and pH on the protein adsorption onto the mixed-mode adsorbents is a complex phenomenon, and it is difficult to develop a theoretical model for predicting such effects. In the present work, an empirical modification of the Langmuir equation is introduced to correlate the adsorption isotherms under varying pH and salt concentrations.

The typical Langmuir equation is

$$Q = \frac{Q_m C}{K_d + C} \quad (1)$$

where  $Q/(\text{mg}\cdot(\text{mL of gel})^{-1})$  is the protein adsorption capacity and  $C/(\text{mg}\cdot\text{mL}^{-1})$  is the protein concentration in the bulk solution. Two parameters, maximum binding capacity  $Q_m/(\text{mg}\cdot(\text{mL of gel})^{-1})$  and the dissociation coefficient  $K_d/(\text{mg}\cdot\text{mL}^{-1})$ , can be considered as the apparent Langmuir parameters, which are functions of salt concentration and pH.

Based on our experimental results,  $Q_m$  and  $K_d$  are approximately exponential functions of salt concentration and pH. Therefore,  $Q_m$  and  $K_d$  are described as follows:

$$Q_m = \exp(aC_s - bC_{[H^+]})Q_{m0} \quad (2)$$

and

$$K_d = \exp(bC_{[H^+]} - aC_s)K_{d0} \quad (3)$$

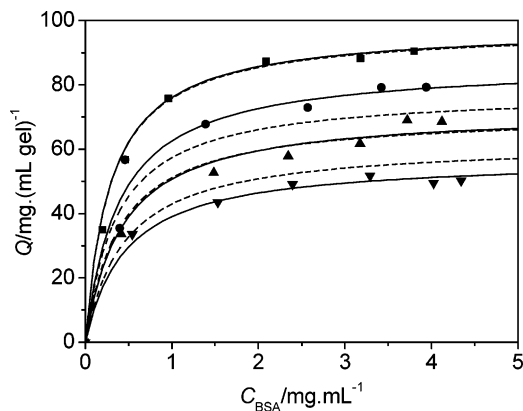


**Figure 1.** Effect of sodium chloride concentration ( $C_s$ ) on the adsorption equilibrium of BSA onto Cell-SSP-BA-1 (ligand density of  $120 \mu\text{mol}\cdot(\text{mL of gel})^{-1}$ ) at pH 7.0 and  $25 \text{ }^\circ\text{C}$ :  $\blacksquare$ ,  $C_s = 0 \text{ mol}\cdot\text{L}^{-1}$ ;  $\bullet$ ,  $C_s = 0.25 \text{ mol}\cdot\text{L}^{-1}$ ;  $\blacktriangle$ ,  $C_s = 0.35 \text{ mol}\cdot\text{L}^{-1}$ ;  $\blacktriangledown$ ,  $C_s = 0.5 \text{ mol}\cdot\text{L}^{-1}$ . Symbols represent experimental data, and solid line and dashed line represent the correlated results with eq 1 and eq 4, respectively.

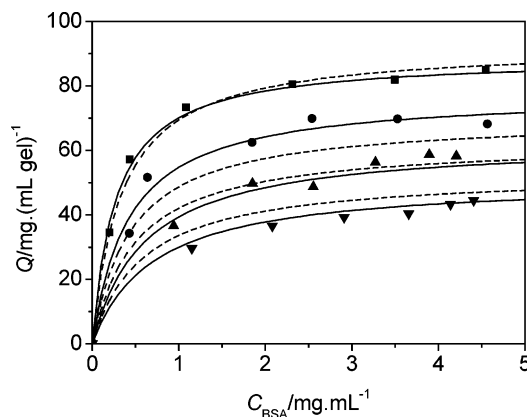


**Figure 2.** Effect of sodium chloride concentration ( $C_s$ ) on the adsorption equilibrium of BSA onto Cell-SSP-BA-2 (ligand density of  $103 \mu\text{mol}\cdot(\text{mL of gel})^{-1}$ ) at pH 7.0 and  $25 \text{ }^\circ\text{C}$ :  $\blacksquare$ ,  $C_s = 0 \text{ mol}\cdot\text{L}^{-1}$ ;  $\bullet$ ,  $C_s = 0.25 \text{ mol}\cdot\text{L}^{-1}$ ;  $\blacktriangle$ ,  $C_s = 0.35 \text{ mol}\cdot\text{L}^{-1}$ ;  $\blacktriangledown$ ,  $C_s = 0.5 \text{ mol}\cdot\text{L}^{-1}$ . Symbols represent experimental data, and solid line and dashed line represent the correlated results with eq 1 and eq 4, respectively.

Then eq 1 can be written as

$$Q = \frac{\exp(aC_s - bC_{[\text{H}^+]})Q_m C}{\exp(bC_{[\text{H}^+] - aC_s)K_d + C} \quad (4)$$

where  $C_s/\text{mol}\cdot\text{L}^{-1}$  is the concentration of sodium chloride in the solution,  $C_{[\text{H}^+]}/\text{mol}\cdot\text{L}^{-1}$  is the concentration of  $\text{H}^+$  in the solution, and  $a/\text{L}\cdot\text{mol}^{-1}$ ,  $b/\text{L}\cdot\text{mol}^{-1}$ ,  $Q_m/\text{mg}\cdot(\text{mL of gel})^{-1}$ , and  $K_d/\text{mg}\cdot\text{mL}^{-1}$  are empirical parameters, which can be determined by fitting the experimental data. Equation 4 is the modified Langmuir equation used in the present work for correlating the influence of both salt concentration and pH on mixed-mode adsorption, which will be discussed in the following section.

**Influence of Salt Concentration on the Mixed-Mode Adsorption.** The adsorption behavior of BSA on the Cell-SSP-BA with different ligand densities was studied under different NaCl concentrations at pH 7.0. The experimental data of isotherm adsorption are given in Table 1, and the isotherm adsorption curves are shown in Figures 1 to 4. The curves were correlated with the Langmuir equation (eq 1), and the apparent maximum binding capacity ( $Q_m$ ) and apparent dissociation coefficient ( $K_d$ ) were obtained and shown in Figure 5. The literature data of Diaion HPA 25,<sup>23</sup> POROS 50 HS,<sup>15</sup> and SP

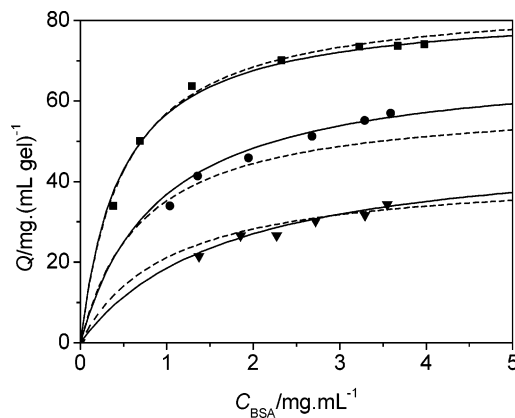


**Figure 3.** Effect of sodium chloride concentration ( $C_s$ ) on the adsorption equilibrium of BSA onto Cell-SSP-BA-3 (ligand density of  $65 \mu\text{mol}\cdot(\text{mL of gel})^{-1}$ ) at pH 7.0 and  $25 \text{ }^\circ\text{C}$ :  $\blacksquare$ ,  $C_s = 0 \text{ mol}\cdot\text{L}^{-1}$ ;  $\bullet$ ,  $C_s = 0.25 \text{ mol}\cdot\text{L}^{-1}$ ;  $\blacktriangle$ ,  $C_s = 0.35 \text{ mol}\cdot\text{L}^{-1}$ ;  $\blacktriangledown$ ,  $C_s = 0.5 \text{ mol}\cdot\text{L}^{-1}$ . Symbols represent experimental data, and solid line and dashed line represent the correlated results with eq 1 and eq 4, respectively.

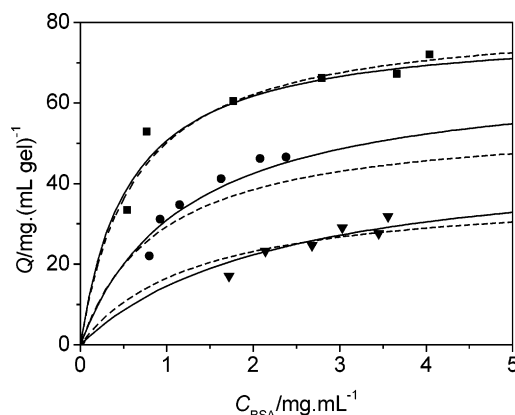


**Figure 4.** Effect of sodium chloride concentration ( $C_s$ ) on the adsorption equilibrium of BSA onto Cell-SSP-BA-4 (ligand density of  $49 \mu\text{mol}\cdot(\text{mL of gel})^{-1}$ ) at pH 7.0 and  $25 \text{ }^\circ\text{C}$ :  $\blacksquare$ ,  $C_s = 0 \text{ mol}\cdot\text{L}^{-1}$ ;  $\bullet$ ,  $C_s = 0.25 \text{ mol}\cdot\text{L}^{-1}$ ;  $\blacktriangle$ ,  $C_s = 0.35 \text{ mol}\cdot\text{L}^{-1}$ ;  $\blacktriangledown$ ,  $C_s = 0.5 \text{ mol}\cdot\text{L}^{-1}$ . Symbols represent experimental data, and solid line and dashed line represent the correlated results with eq 1 and eq 4, respectively.

Sepharose<sup>24</sup> were used for the comparison. As shown in Figures 1 to 4 and Figure 5a, when the salt concentration of the solution increases from (0.0 to 0.5)  $\text{mol}\cdot\text{L}^{-1}$ , the maximum capacity of Cell-SSP-BA-1 decreases from (98 to 57)  $\text{mg}\cdot(\text{mL of gel})^{-1}$ , a capacity loss of about 41.8 %, with 41.6 %, 38.8 %, and 39.2 % loss for Cell-SSP-BA-2, Cell-SSP-BA-3, and Cell-SSP-BA-4, respectively. There is a capacity loss of about 31 % for POROS 50 HS when the salt concentration increases from (0.0 to 0.2)  $\text{mol}\cdot\text{L}^{-1}$ , of 61.2 % for Diaion HPA 25 from (0.0 to 0.05)  $\text{mol}\cdot\text{L}^{-1}$ , and of 44.2 % for SP Sepharose from (0.07 to 0.13)  $\text{mol}\cdot\text{L}^{-1}$ , respectively. The results demonstrated that Cell-SSP-BA adsorbent used in the present work has an obvious property of salt-tolerance. From Figure 5b, it is also evident that the apparent dissociation coefficient  $K_d$  increases with increasing salt concentration and decreasing ligand density. This behavior suggests that the affinity between protein and adsorbent decreases with increasing salt concentration and decreasing ligand density. The differences can be attributed to the interactions between salt ions and protein and between salt ions and adsorbents. The isoelectric point of BSA is about 4.9, and the net charge of the protein surface should be negative at pH 7.0. Under the conditions tested, the adsorption would be promoted due to the electrostatic attraction and hydrophobic interaction between protein and adsorbent. From the relationships between

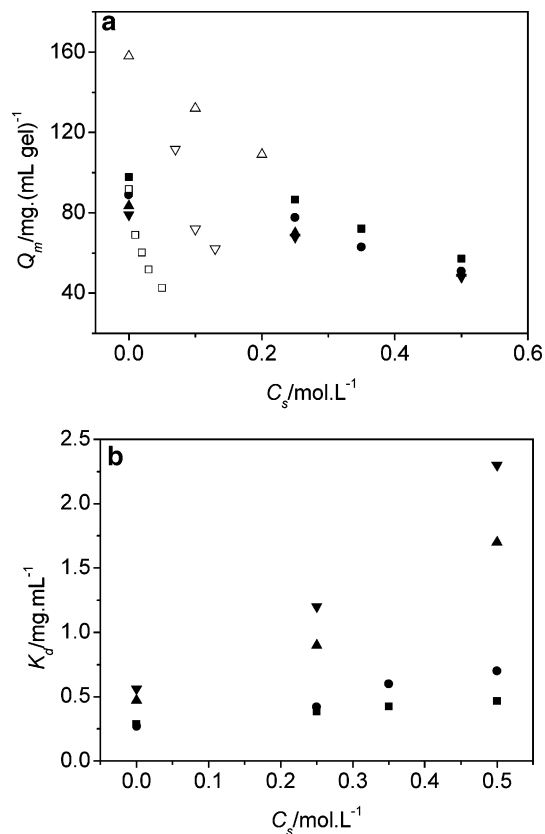


**Figure 5.** Effect of sodium chloride concentration ( $C_s$ ) on the maximum binding capacity ( $Q_m$ ) and apparent dissociation coefficient ( $K_d$ ) at 25 °C correlate by eq 1 for different ligand densities: ■, 120  $\mu\text{mol}\cdot(\text{mL of gel})^{-1}$ ; ●, 103  $\mu\text{mol}\cdot(\text{mL of gel})^{-1}$ ; ▲, 65  $\mu\text{mol}\cdot(\text{mL of gel})^{-1}$ ; ▼, 49  $\mu\text{mol}\cdot(\text{mL of gel})^{-1}$ . Literature data: □, Diaion HPA 25;<sup>23</sup> △, POROS 50 HS;<sup>15</sup> ▽, SP Sepharose.<sup>24</sup>

binding capacity and salt concentration, it appears that the electrostatic interactions are an important influence on protein adsorption for BSA and Cell-SSP-BA systems.

**Influence of pH on the Mixed-Mode Adsorption.** pH is another important factor relative to mixed-mode adsorbent

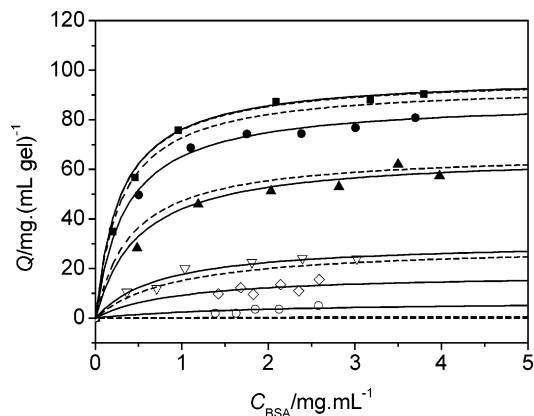


**Figure 6.** Effect of pH on the adsorption equilibrium of BSA onto Cell-SSP-BA-1 (ligand density of 120  $\mu\text{mol}\cdot(\text{mL of gel})^{-1}$ ) at 25 °C: ■, pH 7.0; ●, pH 6.0; ▲, pH 5.0; ▼, pH 4.5; ◇, pH 4.0; ○, pH 3.0. Symbols represent experimental data, and solid line and dashed line represent the correlated results with eq 1 and eq 4, respectively.

behavior. The experimental data of isotherm adsorption at varying pH values are given in Table 2, and the isotherm adsorption curves are shown in Figures 6 to 9. The apparent maximum binding capacity ( $Q_m$ ) and apparent dissociation coefficient ( $K_d$ ) are shown in Figure 10. A pH change mainly could affect the electrostatic interaction between protein and adsorbent by altering the net charge of the protein. As pH values decrease from 7.0 to 5.0, the surface net charge of BSA decreases and thus the adsorption capacity of BSA obviously decreases. As the pH value crosses the isoelectric point of the protein (4.9), the electrostatic charge repulsion interaction becomes significant and it hinders the adsorption of proteins. The adsorbents are positively charged for the pH range investigated because benzylamine ligand has a  $pK_a$  between pH 9.0 and pH 9.5.<sup>7</sup> The results indicate that some BSA adsorption is still occurring even under electrostatic charge repulsion interaction conditions. Two reasons might contribute to this phenomenon. First, the charge distribution on the protein surface is uneven, so the contact regions with negatively charge groups on the protein surface are more favorable for protein interaction

**Table 2. Experimental Results of BSA Adsorption with Cell-SSP-BA at Different pH Values**

$L^a$	pH 6.0		pH 5.0		pH 4.5		pH 4.0		pH 3.0	
	$C$	$Q$	$C$	$Q$	$C$	$Q$	$C$	$Q$	$C$	$Q$
120	0.50	49.6	0.49	28.4	0.37	10.6	1.42	9.8	1.37	2
	1.11	68.7	1.19	46.0	0.71	11.9	1.68	12.2	1.63	2
	1.75	74.2	2.03	51.3	1.04	20.0	1.83	9.6	1.85	3.5
	2.38	74.4	2.82	53.0	1.81	22.5	2.14	13.5	2.12	3.5
	3.01	76.7	3.50	62.1	2.40	24.2	2.35	10.9	2.58	5
	3.70	80.7	3.98	57.5	3.02	24.0	2.59	15.5		
103	0.44	43.3	0.58	29.2	0.37	7.1	1.42	5.1	1.09	0
	1.06	61.3	1.29	39.7	0.58	11.9	1.45	8.2	1.29	0
	1.85	68.2	2.12	44.0	1.04	13.2	1.60	9.6	1.45	1.1
	2.54	68.0	2.75	51.7	1.58	14.1	1.76	10.5	1.76	1.2
	3.32	72.5	3.48	49.5	2.40	20.2	1.95	7.9	1.98	2.5
	3.91	74.1	3.70	57.5	3.02	21.2	1.98	9.5		
65	0.41	25.0	0.66	21.1	0.57	7.0	1.45	3.9	0.69	0
	1.07	47.5	1.08	26.4	1.02	11.2	1.55	5.4	1.05	0.5
	1.86	55.1	1.45	33.8	1.65	11.1	1.68	5.7	1.29	1
	2.83	65.3	2.07	39.3	2.03	12.9	1.74	7.2	1.45	1.2
	3.49	63.5	2.89	42.0	2.64	16.6	1.88	7.2	1.55	1.5
49			0.97	19.4	1.42	8.7	0.56	0		
			1.18	25.6	1.77	9.4	0.80	0.5		
			1.47	30.8	2.27	10.2	1.15	0.6		
			2.21	33.1	2.93	12.5	1.44	0.8		
			2.87	37.3	3.53	13.3				

<sup>a</sup>  $L$  means ligand density.

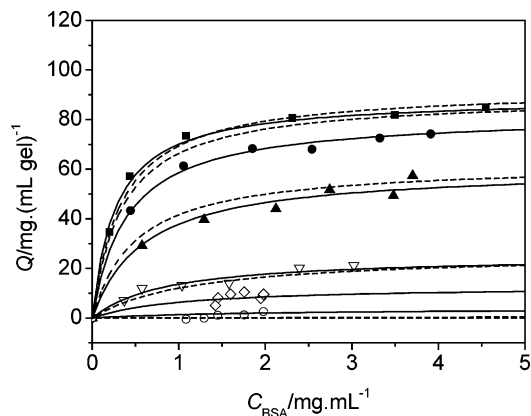


**Figure 7.** Effect of pH on the adsorption equilibrium of BSA onto Cell-SSP-BA-2 (ligand density of  $103 \mu\text{mol}\cdot(\text{mL of gel})^{-1}$ ) at  $25 \text{ }^\circ\text{C}$ : ■, pH 7.0; ●, pH 6.0; ▲, pH 5.0; ▽, pH 4.5; ◇, pH 4.0; ○, pH 3.0. Symbols represent experimental data, and solid line and dashed line represent the correlated results with eq 1 and eq 4, respectively.

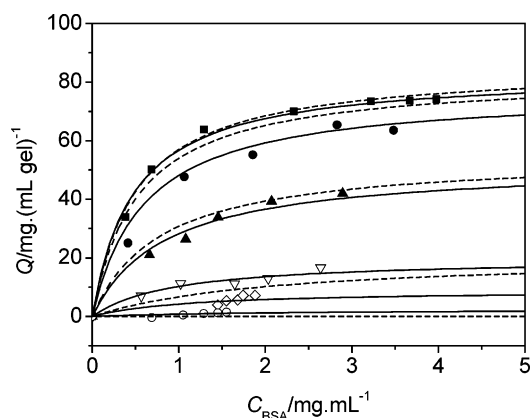


**Figure 8.** Effect of pH on the adsorption equilibrium of BSA onto Cell-SSP-BA-2 (ligand density of  $65 \mu\text{mol}\cdot(\text{mL of gel})^{-1}$ ) at  $25 \text{ }^\circ\text{C}$ : ■, pH 7.0; ●, pH 6.0; ▲, pH 5.0; ▽, pH 4.5; ◇, pH 4.0; ○, pH 3.0. Symbols represent experimental data, and solid line and dashed line represent the correlated results with eq 1 and eq 4, respectively.

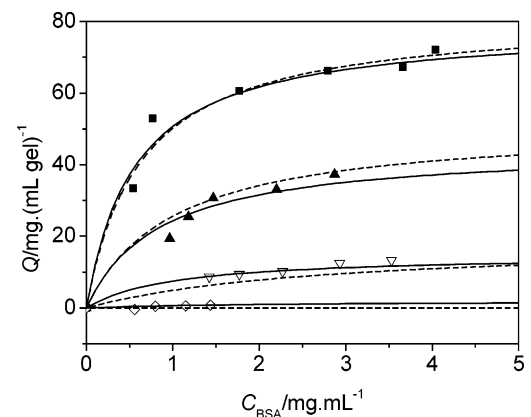


**Figure 9.** Effect of pH on the adsorption equilibrium of BSA onto Cell-SSP-BA-2 (ligand density of  $49 \mu\text{mol}\cdot(\text{mL of gel})^{-1}$ ) at  $25 \text{ }^\circ\text{C}$ : ■, pH 7.0; ▲, pH 5.0; ▽, pH 4.5; ◇, pH 4.0. Symbols represent experimental data, and solid line and dashed line represent the correlated results with eq 1 and eq 4, respectively.

with the positively charged ligand on the adsorbent surface.<sup>25,26</sup> For pH values lower than the protein pI value, the BSA surface still has some negatively charged parts for interaction with the adsorbent so there are still some proteins absorbed. The phenomenon of protein binding to an anion exchanger at pH values below the isoelectric point have also been reported by

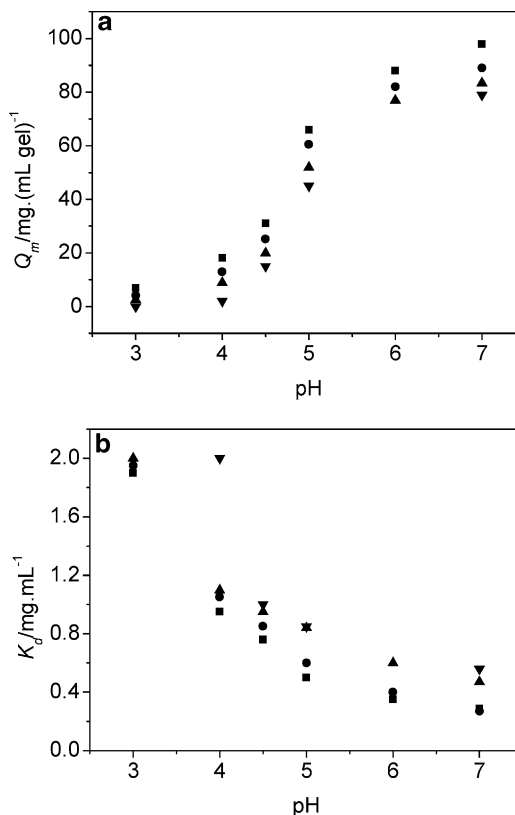


**Figure 10.** Effect of pH on the maximum binding capacity ( $Q_m$ ) and apparent dissociation coefficient ( $K_d$ ) at  $25 \text{ }^\circ\text{C}$  correlated by eq 1 for different ligand densities: ■,  $120 \mu\text{mol}\cdot(\text{mL of gel})^{-1}$ ; ●,  $103 \mu\text{mol}\cdot(\text{mL of gel})^{-1}$ ; ▲,  $65 \mu\text{mol}\cdot(\text{mL of gel})^{-1}$ ; ▼,  $49 \mu\text{mol}\cdot(\text{mL of gel})^{-1}$ .

**Table 3. Parameters Correlated by Equation 4 for BSA Adsorption with Cell-SSP-BA**

$L^a$ $\mu\text{mol}\cdot(\text{mL of gel})^{-1}$	$Q_{m0}$ $\text{mg}\cdot\text{mL}^{-1}$	$K_{d0}$ $\text{mg}\cdot\text{mL}^{-1}$	$a$ $\text{L}\cdot\text{mol}^{-1}$	$b$ $\text{L}\cdot\text{mol}^{-1}$
120	98	0.29	-0.9	$3.8\text{E}+4$
103	93	0.33	-1.1	$4.0\text{E}+4$
65	86	0.50	-1.4	$4.5\text{E}+4$
49	82	0.63	-1.5	$4.7\text{E}+4$

<sup>a</sup> L means ligand density.

other researchers.<sup>26,27</sup> Second, the adsorption or desorption at pH values below the pI depends on the balance between electrostatic charge repulsion and hydrophobic interaction. Therefore, higher ligand density shows a higher binding capacity due to more hydrophobic binding in the adsorbent. This also means that a stronger desorption condition would be required for the higher ligand density adsorbent in the elution process. From Figure 10, it can be observed that the decrease of pH causes the increase of the apparent dissociation coefficient, which means the affinity between protein and adsorbent decreases with decreasing pH values.

**Correlation with the Modified Langmuir Equation.** From Figures 1 to 4 and 6 to 9, it can be observed that the Langmuir equation (eq 1) can fit the experimental adsorption behavior; however, different sets of parameters should be used for varying pH and salt concentration. To correlate the influences of both salt concentration and pH on the mixed-mode adsorption, the Langmuir equation (eq 1) has to be modified, and thus eq 4 is used. The model parameters correlated by eq 4 with the experimental data are listed in Table 3. The correlation results are also shown in Figures 1 to 4 and 6 to 9. It was found that the modified Langmuir equation could provide a good descrip-



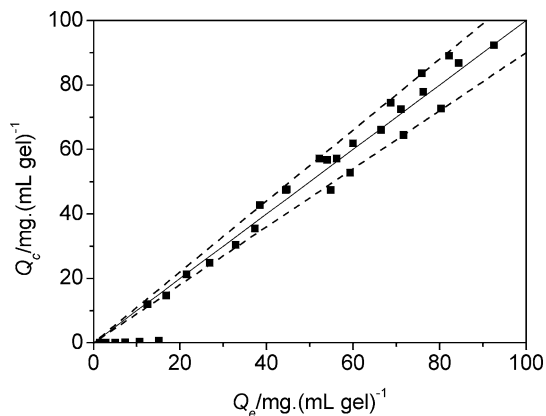


**Figure 11.** Comparison of the calculated adsorption capacity ( $Q_c$ ) and experimental adsorption capacity ( $Q_e$ ). Dashed lines are 10 % uncertainty.

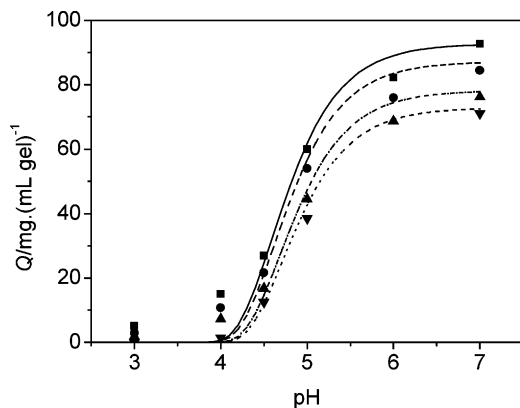


**Figure 12.** Experimental (symbol) and calculated (line) adsorption capacities of BSA with Cell-SSP-BA at 25 °C and 5 mg·mL<sup>-1</sup> protein concentration under varying pH for different ligand densities: ■, —, 120 μmol·(mL of gel)<sup>-1</sup>; ●, ---, 103 μmol·(mL of gel)<sup>-1</sup>; ▲, -·-, 65 μmol·(mL of gel)<sup>-1</sup>; ▼, ···, 49 μmol·(mL of gel)<sup>-1</sup>.

tion of salt concentration and pH dependences on the mixed-mode protein adsorption with only one set of parameters. Figure 11 compares all experimental data with the correlation of eq 4, which demonstrated that the modification of the Langmuir equation in the present work was feasible within  $\pm 10\%$  correlation error. As an example, Figure 12 clearly shows the pH-dependent relationship between experimental values and the calculated results, which show most deviations occur under nonadsorption conditions.

The modified Langmuir equation (eq 4) was challenged further upon using some literature data. Weaver and Carta<sup>15</sup> reported the adsorption isotherms of lysozyme with the ion exchanger POROS 50 HS in Na<sub>2</sub>HPO<sub>4</sub> buffer (pH 6.5) with salt concentrations of (0, 0.1, 0.2, and 0.3) mol·L<sup>-1</sup>, respectively. The adsorbent has the hydrophobic backbones derived from a styrene–divinylbenzene matrix, so some amount of salt-tolerant property could be found. The correlation results obtained using eq 4 are shown in Figure 13. It can be seen that the salt-dependent adsorption behavior can be described up to 0.2 mol·L<sup>-1</sup> NaCl. At higher salt concentrations (0.3 mol·L<sup>-1</sup>), the adsorption becomes less favorable, and the isotherms tend to approach linearity, which cannot be described by eq 4. Bosma and Wesselingh<sup>22</sup> reported the adsorption equilibrium of BSA with Q-Sepharose at different pH values and ionic strength. As shown in Figure 14, the tendency of binding capacity with pH can be well described by eq 4 regardless of the salt concentration. In addition, the tendency described by eq 4 cannot be used at extreme pH conditions (e.g.,

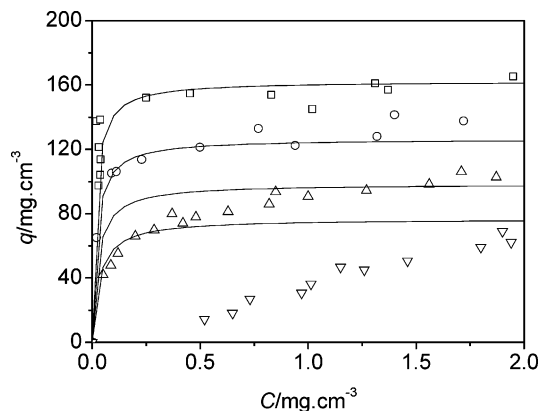


**Figure 13.** Equilibrium uptake of lysozyme by POROS 50 HS in 0.01 mol·L<sup>-1</sup> Na<sub>2</sub>HPO<sub>4</sub> buffer at pH 6.5 with different NaCl concentrations:<sup>15</sup> □, 0 mol·L<sup>-1</sup> NaCl; ○, 0.1 mol·L<sup>-1</sup> NaCl; △, 0.2 mol·L<sup>-1</sup> NaCl; ▽, 0.3 mol·L<sup>-1</sup> NaCl. Solid line represent the results calculated by eq 4.

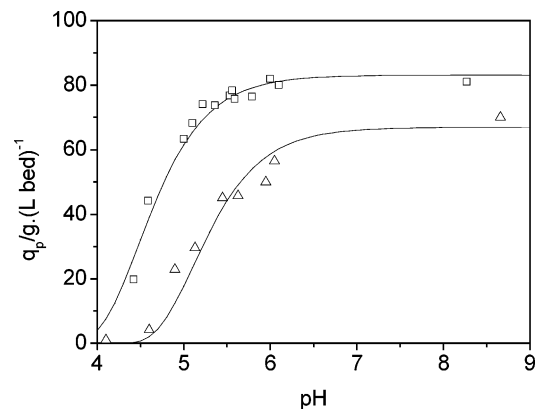


**Figure 14.** Measured and calculated adsorption capacities of BSA on Q-Sepharose FF at 25 °C and 12 g·L<sup>-1</sup> total protein concentration under varying pH and ionic strength:<sup>22</sup> □, 0.008 mol·L<sup>-1</sup>; △, 0.04 mol·L<sup>-1</sup>; The solid lines (—) are correlated by eq 4 regardless of salt concentrations.

pH 10 to pH 14) because binding capacity would decrease at such pH values due to the competition of adsorption between the protein ions and the large number of negative ions in the solution.<sup>28</sup>

## Conclusions

With BSA as the model protein, adsorption isotherm curves with the mixed-mode adsorbent Cell-SSP-BA were measured for different ligand densities. The protein binding behavior showed some typical properties, such as salt-tolerance and pH dependence. At moderate salt concentration, relatively high binding capacity could be achieved. The results indicated that electrostatic interactions might be an important contributor to the protein adsorption for this system. Also, the results showed a high ligand density results in high binding capacity and high affinity with proteins. However, harsher elution conditions would be necessary for the desorption procedure.

The Langmuir equation was modified to correlate the dependence of both salt concentration and pH value on the equilibrium adsorption of proteins to the mixed-mode adsorbent. The modified Langmuir equation provided a good fit of the experimental data, excepting unfavorable adsorption, which could be used to predict the influences of salt concentration and pH on the mixed-mode protein adsorption. Further studies in this field are needed to describe accurately the specific adsorption behavior and improve the application of mixed-mode adsorption technologies.

## Literature Cited

- (1) Hofstee, B. J. J. Protein binding by agarose carrying hydrophobic groups in conjunction with charges. *Biochem. Biophys. Res. Commun.* **1973**, *50*, 751–757.
- (2) Yon, R. J.; Simmonds, R. J. Protein chromatography on adsorbents with hydrophobic and ionic groups. *Biochem. J.* **1975**, *151*, 281–290.
- (3) Sasaki, I.; Gotoh, H.; Yamamoto, R.; Tanaka, H.; Takami, K.; Yamashita, K.; Yamashita, J.; Horio, T. Hydrophobic-ionic chromatography: its application to microbial glucose oxidase, hyaluronidase, cholesterol oxidase and cholesterol esterase. *Biochem. J.* **1982**, *91*, 1555–1561.
- (4) Burton, S. C.; Harding, D. R. K. Salt-independent adsorption chromatography new broad-spectrum affinity methods for protein capture (review). *J. Biochem. Biophys. Methods* **2001**, *49*, 275–287.
- (5) Burton, S. C.; Haggarty, N. W.; Harding, D. R. K. One step purification of chymosin by mixed mode chromatography. *Biotechnol. Bioeng.* **1997**, *56*, 45–55.
- (6) Lu, M.-H.; Lin, D.-Q.; Wu, Y.-C.; Yun, J.-X.; Mei, L.-H.; Yao, S.-J. Separation of nattokinase from *Bacillus subtilis* fermentation broth by expanded bed adsorption with mixed-mode adsorbent. *Biotechnol. Bioprocess Eng.* **2005**, *10*, 128–135.
- (7) Hamilton, G. E.; Leuchau, F.; Burton, S. C.; Lyddiatt, A. Development of a mixed mode adsorption process for the direct product sequestration of an extracellular protease from microbial batch cultures. *J. Biotechnol.* **2000**, *79*, 103–115.
- (8) Ghose, S.; Hubbard, B.; Cramer, S. M. Protein interactions in hydrophobic charge induction chromatography (HCIC). *Biotechnol. Prog.* **2005**, *21*, 498–508.
- (9) Lei, Y.-L.; Lin, D.-Q.; Yao, S.-J.; Zhu, Z.-Q. Preparation and characterization of titanium oxide-densified cellulose beads for expanded bed adsorption. *J. Appl. Polym. Sci.* **2003**, *90*, 2848–2854.
- (10) Lei, Y.-L.; Lin, D.-Q.; Yao, S.-J.; Zhu, Z.-Q. Preparation of an anion exchanger based on TiO<sub>2</sub>-densified cellulose beads for expanded bed adsorption. *React. Funct. Polym.* **2005**, *62*, 169–177.
- (11) Miao, Z.-J.; Lin, D.-Q.; Yao, S.-J. Preparation and characterization of cellulose-stainless steel powder composite particles customized for expanded bed application. *Ind. Chem. Eng. Res.* **2005**, *44*, 8218–8224.
- (12) Lin, D.-Q.; Miao, Z.-J.; Yao, S.-J. Expansion and hydrodynamic properties of cellulose–stainless steel powder composite matrix for expanded bed adsorption. *J. Chromatogr. A* **2006**, *1107*, 265–272.
- (13) Gao, D.; Yao, S.-J.; Lin, D.-Q. Preparation and adsorption behavior of cellulose-based mixed-mode adsorbent with benzylamine ligand for expanded bed application. *Ind. Chem. Eng. Res.* In revision.
- (14) Burton, S. C.; Harding, D. R. K. Hydrophobic charge induction chromatography salt independent protein adsorption and facile elution with aqueous buffers. *J. Chromatogr. A* **1998**, *814*, 71–81.
- (15) Weaver, L. E., Jr.; Carta, G. Protein adsorption on cation exchangers: comparison of macroporous and gel-composite media. *Biotechnol. Prog.* **1996**, *12*, 342–356.
- (16) Fausnaugh, J. L.; Regnier, F. E. Solute and mobile phase contributions to retention in hydrophobic interaction chromatography of proteins. *J. Chromatogr.* **1986**, *359*, 131–146.
- (17) Skidmore, G. L.; Horstmann, B. J.; Chase, H. A. Modelling single-component protein adsorption to the cation exchanger S sepharose FF. *J. Chromatogr.* **1990**, *498*, 113–128.
- (18) Whitley, R. D.; Wachter, R.; Liu, F.; Wang, N.-H. Ion-exchange equilibria of lysozyme, myoglobin and bovine serum albumin. *J. Chromatogr.* **1989**, *465*, 137–156.
- (19) Hu, S.-G.; Do, D. D.; Hossain, M. M. Step elution in preparative liquid chromatography. *J. Chromatogr.* **1992**, *605*, 175–191.
- (20) James, E. A.; Do, D. D. Equilibria of biomolecules on ion-exchange adsorbents. *J. Chromatogr.* **1991**, *542*, 19–28.
- (21) Brooks, C. A.; Cramer, S. M. Steric mass action ion-exchange: displacement profiles and induced salt gradients. *AIChE J.* **1992**, *38*, 1969–1978.
- (22) Bosma, J. C.; Wesselingh, J. A. pH dependence of ion-exchange equilibrium of proteins. *AIChE J.* **1998**, *44*, 2399–2409.
- (23) Lan, Q.-D.; Bassi, A. S.; Zhu, J.-X.; Margaritis, A. A modified Langmuir model for the prediction of the effects of ionic strength on the equilibrium characteristics of protein adsorption onto ion exchange/affinity adsorbents. *Chem. Eng. J.* **2001**, *81*, 179–186.
- (24) Hashim, M. A.; Chu, K. H.; Tsan, P. S. Effects of ionic strength and pH on the adsorption equilibria of lysozyme on ion exchangers. *J. Chem. Technol. Biotechnol.* **1995**, *62*, 253–260.
- (25) Regnier, F. E. The role of protein structure in chromatographic behavior. *Science* **1987**, *238*, 319–323.
- (26) Shi, Q.-H.; Zhou, Y.; Sun, Y. Influence of pH and ionic strength on the steric mass-action model parameters around the isoelectric point of protein. *Biotechnol. Prog.* **2005**, *21*, 516–523.
- (27) Lin, F.-Y.; Chen, C.-S.; Chen, W.-Y.; Yamamoto, S. Microcalorimetric studies of the interactions mechanisms between proteins and Q-Sepharose at pH near pI: effects of NaCl concentrations, pH values, and temperature. *J. Chromatogr. A* **2001**, *912*, 281–289.
- (28) Huang, J.-X.; Schudel, J.; Guiochon, G. Adsorption behaviour of albumin and conalbumin on TSK-DEAE 5PW anion exchanger. *J. Chromatogr.* **1990**, *504*, 335–349.

Received for review December 20, 2005. Accepted April 7, 2006. The financial support of the National Natural Science Foundation of China is gratefully acknowledged.

JE050528P